Combined analytical and numerical approach to magnetization plateaux in one-dimensional spin tube antiferromagnets

X. Plat, S. Capponi, and P. Pujol

Laboratoire de Physique Théorique, IRSAMC, CNRS and Université de Toulouse, UPS, F-31062 Toulouse, France

(Received 21 March 2012; published 16 May 2012)

In this paper, we investigate the properties of frustrated three-leg spin-S tubes under a magnetic field. We concentrate on two kind of geometries for these tubes, one of which is relevant for the compound $[(CuCl_2tachH)_3Cl]Cl_2$. We perform an analytical large-S path-integral approach to determine the phase diagrams, which exhibit several magnetization plateaux. Moreover, by combining the field-theory approach with a strong-coupling one, we also investigate the issue of gapless nonmagnetic excitations on some plateaux, dubbed chirality degrees of freedom for both tubes: on increasing the intertriangle exchange couplings, a gapless chiral phase transforms into a gapped "ferrochiral" state, possibly through intermediate "spin-imbalanced" states. All these predictions are confirmed numerically using large-scale density-matrix renormalization-group simulations for the $S = 3/2$ case.

DOI: 10.1103/PhysRevB.85.174423 PACS number(s): 71.10.Pm, 75.60.−d

I. INTRODUCTION

Nowadays, one-dimensional and quasi-one-dimensional antiferromagnetic (AF) quantum spin systems are a very active theme in condensed matter physics. Thanks to efforts in chemical synthesis, it is now possible to obtain materials which can be effectively considered as one-dimensional systems, making it possible to verify the theoretical predictions.

The natural extensions of quantum spin chains are quantum spin ladders, which are made of two or more coupled chains. These ladders represent the first step between one- and two-dimensional systems. They give rise to interesting features[1] and have been extensively studied over the last decades. So far, various properties have been established both analytically and experimentally.[2–8] Going back to the problem of a single Heisenberg spin-S chain, we know since the work of Haldane[9] that the chain is gapless (respectively gapped) if S is half-integer (respectively integer). In a similar way, there is a parity effect of the number of coupled half-integer spin chains to form the ladder.[10] A gap opens in the spectrum of antiferromagnetic spin ladders with an even number of legs, and their spin correlation functions decay exponentially. On the other hand, for an odd number of legs of half-integer spin, such ladders have massless excitations above their ground state and the decay of the spin correlations is algebraic. Experimental investigations have confirmed these predictions, for example, the observation of a gap in the spin-1/2 two-leg ladders $SrCu_2O_3$ (Ref. 11) and $Cu_2(C_5H_{12}N_2)_2Cl_4$.[12]

New properties arise when the role of transverse boundary conditions is taken into account. The results quoted above are valid only for ladders, which correspond to open boundary condition (OBC). Applying periodic boundary conditions (PBC) in the rung direction to form a spin tube seems to cause the opening of a gap in both even and odd cases. For an even number of legs, this is explained in terms of the formation of spin singlets in the transverse direction. The reason is different in the odd case, where the PBC induce geometrically frustrated interactions. The direct consequence of this frustration is a twofold-degenerate dimerized ground state with an excitation gap above it.[13] A recent review for the spin tube has been published in Ref. 14.

Among the questions emerging from the study of these quasi-one-dimensional systems, an important one concerns their magnetization process when an external magnetic field is turned on. Classically, the magnetization curve of such systems is expected to be a straight line until the saturation field. But, at low enough temperatures, quantum effects begin to play a role and magnetization plateaux can appear. This has been observed in various chains and ladders spin systems.[15–18]

A condition, neither sufficient nor necessary, for the existence of magnetization plateaux in a quantum spin-S chain has been found by Oshikawa, Yamanaka, and Affleck (OYA).[19] This condition, which was later extended to ladder systems,[6] restricts the possible values of the magnetization for a plateau. It reads as

$$N(S - m) \in \mathbb{Z}, \tag{1}$$

where m is the onsite magnetization and N the number of spins per unit cell. This result has been obtained through a generalization of the Lieb-Schultz-Mattis (LSM) theorem.[20] Although the low-energy state constructed in this approach has the same total magnetization as the ground state, they present bosonization arguments indicating that, in general, low-energy states appear also in different magnetization sectors. In 2009, Tanaka, Totsuka, and Hu (TTH) have used a spin coherent-states path-integral approach to recover this condition.[21] The main advantage of their method is that it can be applied for any value S.

In this paper, we investigate successively the effect of a magnetic field on two different types of three-leg spin tubes of spin S, namely, the simple spin tube and the twisted spin tube, which will be described below. For each one, we combine analytical and numerical methods and proceed as follows. First, we apply to the spin tube the TTH approach, which takes into account the effects of the Berry phase appearing in the partition function. This leads to an effective field theory for the spin tube, from which a condition on the magnetization plateaux is inferred and we give an estimate of the region of existence of the plateaux. We also discuss the question of having gapless nonmagnetic excitations, but also several different gapped phases for these excitations. Then, in the case

of half-integer spins, we study the limit of strongly coupled chains. A new nonmagnetic degree of freedom appears in this regime for the magnetizations of the lowest and highest magnetization plateaux, namely, a right or left chirality. It comes from the twofold degeneracy of the ground state. In this limit, we show the possibility of the existence on those plateaux of a quantum phase transition. As the coupling along the chains is increased, the chirality degree of freedom may go from a critical to a gapped regime. This behavior has recently been observed in the simple spin tube of spin-1/2 by Okunishi *et al*. using density-matrix renormalization-group (DMRG) calculations.[22] We expect this transition to be well accounted by a perturbated XXZ effective Hamiltonian and support this statement by a very simple qualitative numerical result. Then, we perform DMRG calulations to study the magnetization process. Analyzing the entanglement entropy and the local magnetizations, we finally examine the different phases occurring for the chirality on the plateaux.

The rest of the paper is organized as follows. In Sec. II, we consider the case of the simple three-leg spin tube by using the path-integral approach to understand the appearance of some magnetization plateaux, then we investigate the role of the chirality degrees of freedom, and finally we compare our predictions to DMRG simulations in the $S = 3/2$ case. In Sec. III, the case of the twisted spin tube is addressed following the same strategy. Finally, we draw some conclusions and discuss possible perspectives in Sec. IV. Some technical details about the duality transformation are given in an Appendix.

II. SIMPLE SPIN TUBE

A. The model

The Hamiltonian of the simple spin tube, which is the first geometry that we consider, reads as

$$\begin{aligned} H &= H_\perp + H_\parallel + H_h, \\ H_\perp &= J_\perp \sum_j \sum_{\alpha=1,2,3} \vec{S}_{\alpha,j} \cdot \vec{S}_{\alpha+1,j}, \\ H_\parallel &= J_\parallel \sum_j \sum_{\alpha=1,2,3} \vec{S}_{\alpha,j} \cdot \vec{S}_{\alpha,j+1}, \\ H_h &= -h \sum_j \sum_{\alpha=1,2,3} S^z_{\alpha,j}, \end{aligned} \tag{2}$$

where $\vec{S}_{\alpha,j}$ is the spin-S operator, $J_\parallel > 0$ is the intrachain AF coupling, $J_\perp > 0$ the AF rung coupling, and h the magnetic field along the z axis (Fig. 1). The subscript i (α) represents the site number in the chain (rung) direction. The tube structure (PBC in the rung direction) induces frustration in this simple nearest-neighbor model. Applied to this model, the OYA condition (1) takes the form

$$3(S - m) \in \mathbb{Z}, \tag{3}$$

as there are three spins per unit cell.

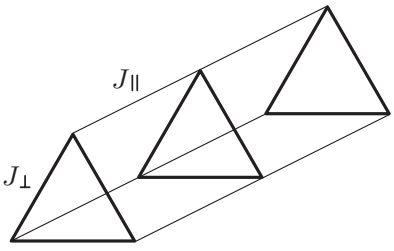

FIG. 1. Lattice structure of the simple spin tube.

So far, the Hamiltonian (2) has already been investigated in previous works. By using bosonization techniques for the spin $S = 1/2$ and in zero magnetic field, Schulz has suggested that the tube has a spin gap induced by the geometric frustration.[23] DMRG calculations have confirmed this statement by establishing the existence of a spin gap,[13] which is explained in terms of a twofold-degenerate dimerized ground state with broken translation symmetry. New questions arise when one of the couplings between the rungs is changed, making the tube asymmetric. In that case, it seems that the spin gap vanishes for a small but finite asymmetry.[24] The effect of a magnetic field has also been addressed.[25–29] For higher half-integer spins, only a few results are available. In the $S = 3/2$ case, the existence of a spin gap, as for $S = 1/2$, has been reported recently.[30] Moving to integer spins S, the simple spin tube displays interesting properties. For weakly coupled chains, another parity effect has been established for the low-energy properties using the nonlinear sigma model (NLSM). For an odd number of legs, the lowest magnon band of the model (2) is sixfold degenerate, compared to the threefold degeneracy of nonfrustrated systems, namely, tubes with an even number of legs or ladders.[31–33] Turning on a uniform or nonuniform magnetic field, Sato predicted a succession of quantum phase transitions between critical phases as the field is increased, along with again an even-odd effect.[31] Introducing an asymmetry in the rung couplings, a NLSM analysis and DMRG results have shown the existence of $2S$ quantum phase transitions between gapped phases when varying the anisotropy parameter.[34]

Finally, we discuss the *classical configurations* of the spin tube (2). For decoupled triangles with no external field, the three spins are simply lying in the same plane with angles of $2\pi/3$ between them. If the triangles are now coupled by the $J_\parallel$ term, the situation does not change as the longitudinal coupling is not frustrating and satisfied with a $k_\parallel = \pi$ order in this direction. A magnetic field arranges the spins in an "umbrella" configuration, where the three spins on the triangle are equally polarized and have angles of $2\pi/3$ between their projections in the plane. Thus, the classical ground state of the simple spin tube is simply an umbrella configuration on each triangle with a canted order along the tube. We parametrize it as

$$\vec{S}_{\alpha,j} = S \begin{pmatrix} (-1)^j \sin(\theta_0)\cos\left(\varphi^0_\alpha\right) \\ (-1)^j \sin(\theta_0)\sin\left(\varphi^0_\alpha\right) \\ \cos(\theta_0) \end{pmatrix}, \tag{4}$$

where $\cos(\theta_0) = \frac{h}{S(3J_\perp + 4J_\parallel)}$ and $\varphi^0_\alpha = (\alpha - 1)2\pi/3$.

This state breaks the U(1) symmetry around the z axis, one-site translations, and parity transformations. More precisely, the last one is a symmetry which is going to play a very important role in this system. It is related to what we dub the chirality degree of freedom. Consider the chirality vector order

parameter

$$\chi_j = \frac{1}{3}\sum_{\alpha=1}^{3}(\vec{S}_{\alpha,j}\times\vec{S}_{\alpha+1,j})^z, \tag{5}$$

which is invariant under cyclic permutation of the three chain indices (i.e., translations in the transverse directions) but changes sign under the permutation of two chains. For the classical configuration (4), it reads as $\chi_j \propto \sum_\alpha \sin[(\varphi^0_\alpha - \varphi^0_{\alpha+1})/2]$. Thus, the choice of a given classical configuration, namely, the choice of $\varphi^0_\alpha - \varphi^0_{\alpha+1} = \pm 2\pi/3$, fixes the sign of this order parameter and breaks the $\mathbb{Z}_2$ symmetry explicitly. This in turn will have important consequences in the analysis of the chirality behavior within the path-integral approach.

B. Path-integral approach

1. Derivation of a low-energy action

We begin the study of the simple spin tube (2) following the method recently developed by Tanaka, Totsuka, and Hu.[21] They used a Haldane's spin coherent-state[35] path-integral approach to rederive the OYA condition (1) for the Heisenberg chain with easy-plane single-ion anisotropy. Haldane's analysis leads to an action comprising two terms. One is the coherent-state expectation value of the Hamiltonian, or simply the Hamiltonian for the classical configuration. The other term is the Berry phase one and corresponds to the surface area (or the solid angle) $\int d\tau\{1-\cos[\theta(\tau)]\}\partial_\tau\varphi(\tau)$ in spherical coordinates, enclosed by each spin during its imaginary-time τ evolution. We want to build a low-energy effective theory from this starting point. The method consists in finding the classical ground state of the system and then adding the quantum fluctuations to derive an effective action. The interest of the method is its validity for any value of the spin S. Indeed, while this approach is designed for large-S values, the topological nature of the Berry phase makes the results robust even for smaller S.

We start from the classical ground state discussed in Sec. II A and now we add the fluctuations around this state, writing

$$\begin{cases}\theta_0 \to \theta_{\alpha,j} = \theta_0 + \delta\theta_{\alpha,j},\\ \varphi^0_\alpha \to \varphi^0_\alpha + \varphi_{\alpha,j} = (\alpha-1)\frac{2\pi}{3} + \varphi_{\alpha,j},\end{cases} \tag{6}$$

and expand the spin components up to second order in $\delta\theta$. The calculation of the SU(2) commutation relations $[S^z_{\alpha,i}, S^\pm_{\beta,j}]$ leads to introducing a new set of variables $\Pi_{\alpha,j}$, defined by

$$\Pi_{\alpha,j} = -S\left[\sin(\theta_0)\delta\theta_{\alpha,j} + \tfrac{1}{2}\cos(\theta_0)\delta\theta^2_{\alpha,j}\right], \tag{7}$$

which are the conjugates of the $\varphi_{\alpha,j}$'s. It ensures to have the correct commutators for the spin operators. Then, we rewrite these operators as functions of the conjugate fluctuation variables $\varphi_{\alpha,j}$ and $\Pi_{\alpha,j}$ as

$$\begin{cases} S^\pm_{\alpha,j} \approx (-1)^j e^{\pm i[(\alpha-1)\frac{2\pi}{3}+\varphi_{\alpha,j}]} S\left[\sin(\theta_0) - \dfrac{m}{S^2\sin(\theta_0)}\Pi_{\alpha,j} - \dfrac{1}{2}\dfrac{S^2}{S^2-m^2}\dfrac{1}{S^2\sin(\theta_0)}\Pi^2_{\alpha,j}\right],\\ S^z_{\alpha,j} \approx S\cos(\theta_0) + \Pi_{\alpha,j},\end{cases} \tag{8}$$

where $m = S\cos(\theta_0)$ is the classical magnetization per site.

Casting these expressions into the action, taking the continuum limit, and keeping terms up to second order in the fields, we obtain the low-energy effective action

$$\begin{aligned} S[\{\Pi_\alpha\},\{\varphi_\alpha\}] = \int d\tau\, dx \Bigg\{ &\sum_{\alpha=1,2,3}\left[\frac{1}{2}aJ_\parallel(S^2-m^2)(\partial_x\varphi_\alpha)^2 + a\left(2J_\parallel + \frac{1}{2}J_\perp\frac{S^2}{S^2-m^2}\right)\Pi^2_\alpha\right]\\ &+ aJ_\perp\left(1-\frac{1}{2}\frac{m^2}{S^2-m^2}\right)(\Pi_1\Pi_2+\Pi_2\Pi_3+\Pi_3\Pi_1) + \frac{J_\perp}{4}\frac{S^2-m^2}{a}[(\varphi_1-\varphi_2)^2+(\varphi_2-\varphi_3)^2+(\varphi_3-\varphi_1)^2]\\ &- \frac{\sqrt{3}}{2}mJ_\perp[\Pi_1(\varphi_3-\varphi_2)+\Pi_2(\varphi_1-\varphi_3)+\Pi_3(\varphi_2-\varphi_1)] + i\sum_{\alpha=1,2,3}\left[\left(\frac{S-m}{a}\right)\partial_\tau\varphi_\alpha - \Pi_\alpha\partial_\tau\varphi_\alpha\right]\Bigg\}, \end{aligned} \tag{9}$$

with a the lattice constant. We see that all the fluctuations, transverse or longitudinal, are coupled. The last two imaginary terms come from the Berry phase part of the action. It is important to stress that the $\partial_\tau\varphi_\alpha$ terms, although being total derivatives, can not be dropped. Indeed, the fields φ_α are angular variables defined on a circle and thus this term counts the winding number of each field.

As at this order the action is Gaussian in the fields Π_α, we can integrate them out and the action becomes

$$\begin{aligned} S[\{\phi_\alpha\}] &= S_{ch}[\phi_1,\phi_2] + S_s[\phi_s],\\ S_{ch}[\phi_1,\phi_2] &= \int d\tau\, dx\left\{\frac{1}{2}\lambda^{(1,2)}_\tau[(\partial_\tau\phi_1)^2+(\partial_\tau\phi_2)^2] + \frac{1}{2}\lambda^{(1,2)}_x[(\partial_x\phi_1)^2+(\partial_x\phi_2)^2] + M^2(\phi_1^2+\phi_2^2) - i\mu(\phi_1\partial_\tau\phi_2 - \phi_2\partial_\tau\phi_1)\right\},\\ S_s[\phi_s] &= \int d\tau\, dx\left\{\frac{1}{2}\lambda^{(s)}_\tau(\partial_\tau\phi_s)^2 + \frac{1}{2}\lambda^{(s)}_x(\partial_x\phi_s)^2 + i3\frac{S-m}{a}\partial_\tau\phi_s\right\}, \end{aligned} \tag{10}$$

where S_{ch} denotes, for reasons which will become clear later, the chirality part of the action and S_s the symmetric one. We have made the change of variable $\vec{\phi} = U\vec{\varphi}$, where

$$\vec{\phi} = \begin{pmatrix} \phi_1 \\ \phi_2 \\ \phi_s \end{pmatrix}, \quad \vec{\varphi} = \begin{pmatrix} \varphi_1 \\ \varphi_2 \\ \varphi_s \end{pmatrix}, \quad U = \begin{pmatrix} -\frac{1}{\sqrt{2}} & \frac{1}{\sqrt{2}} & 0 \\ -\frac{1}{\sqrt{6}} & -\frac{1}{\sqrt{6}} & \frac{2}{\sqrt{6}} \\ \frac{1}{\sqrt{3}} & \frac{1}{\sqrt{3}} & \frac{1}{\sqrt{3}} \end{pmatrix}, \tag{11}$$

and have rescaled the symmetric field as $\phi_s \to \phi_s/\sqrt{3}$. The coefficients of the action (10) read as

$$\begin{aligned} &\lambda_\tau^{(1,2)} = \frac{1}{a\left(4J_\parallel + \frac{3}{2}J_\perp \frac{m^2}{S^2-m^2}\right)}, \quad \lambda_\tau^{(s)} = \frac{3}{a(4J_\parallel + 3J_\perp)}, \quad \lambda_x^{(1,2)} = aJ_\parallel(S^2-m^2), \quad \lambda_x^{(s)} = 3aJ_\parallel(S^2-m^2), \\ &M^2 = 3J_\parallel J_\perp \frac{S^2-m^2}{a\left(4J_\parallel + \frac{3}{2}J_\perp \frac{m^2}{S^2-m^2}\right)}, \quad \mu = \frac{3}{2}J_\perp \frac{m}{a\left(4J_\parallel + \frac{3}{2}J_\perp \frac{m^2}{S^2-m^2}\right)}. \end{aligned} \tag{12}$$

The symmetric field is now decoupled from ϕ_1 and ϕ_2, and we will study them separately.

2. *Symmetric action and magnetization plateaux*

We notice that the action S_s for the ϕ_s field obtained in Eq. (10) has the same form as the action of the Heisenberg chain in a magnetic field.[21] The term $i\partial_\tau\phi_s$ comes directly from the Berry phase part of the action discussed above. In order to understand its role on the low-energy physics, we apply a duality transformation[36] on this action (details are given in the Appendix). The dual action finally reads as

$$\begin{aligned} S[\tilde{\Phi}_s] = \int d\tau\, dx \Big\{ &\frac{1}{2}K_s(\vec{\nabla}\tilde{\Phi}_s)^2 \\ &+ g_1 \cos\left(2\pi\left[\tilde{\Phi}_s + 3\frac{S-m}{a}x\right]\right)\Big\}, \end{aligned} \tag{13}$$

where $\tilde{\Phi}_s$ is the dual field, $K_s = 1/\sqrt{\lambda_\tau^{(s)}\lambda_x^{(s)}}$, $\vec{\nabla} = (\partial_\tau, \partial_x)$, and g_1 is a constant we have not computed.

We find a Gaussian action perturbed by a cosine term. It is the sine-Gordon action in $(1+1)$ dimensions plus a spatial modulation $2\pi 3(S-m)x/a$ of the cosine. This modulation is a direct consequence of the topological Berry phase. We can therefore separate two cases. If $3(S-m) \notin \mathbb{Z}$, the cosine is incommensurate and will average to zero by integrating over space. It remains a simple gapless Gaussian model and there will not be any plateau in the magnetization curve for general values of m. We can understand the effect of the Berry phase in terms of protecting the system from the vortices. On the other hand, if

$$3(S-m) \in \mathbb{Z}, \tag{14}$$

the cosine is commensurate and we recover the sine-Gordon model. A gap can open in the spectra, causing the emergence of plateaux in the magnetization curve for these particular magnetizations. For example, we expect to observe a plateau for average magnetization per site 1/6, 1/2, 5/6, and 7/6 in the $S = 3/2$ case.

More precisely, the presence of the cosine term is not sufficient to open a gap. It has to be relevant in the renormalization-group (RG) sense and it will depend on the microscopic parameters. From the well-known action (13)

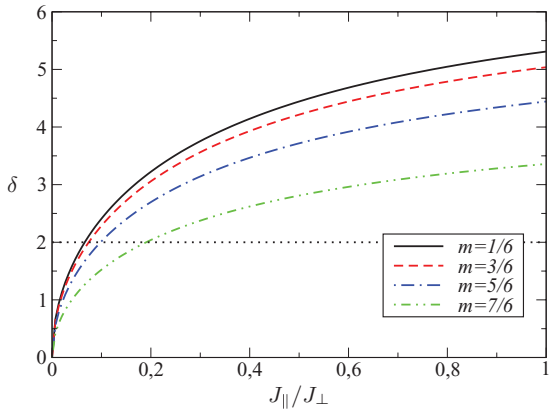

FIG. 2. (Color online) Scaling dimension δ of the cosine operator in the action (13) as a function of $J_\parallel/J_\perp$ for $S = 3/2$ at the values of m fulfilling the condition (14). The perturbation is relevant and opens a gap in the spectrum if $\delta < 2$, thus the plateaux should disappear for $J_\parallel/J_\perp \gtrsim 0.1$.

(without modulation), we compute the scaling dimension δ:

$$\delta = \pi \sqrt{\frac{3J_\parallel(S^2-m^2)}{J_\perp\left(1+\frac{4J_\parallel}{3J_\perp}\right)}}. \tag{15}$$

For the cosine term to be relevant, δ has to be smaller than 2 and thus we expect plateaux in the weakly coupled triangles regime (see Fig. 2 for S = 3/2).

We end this discussion with some comments. First, it is worth noting that the condition (14) does not predict the $m = 0$ plateau found numerically by DMRG.[13] But, in the action (13), higher harmonics of the cosine term have been dropped, especially the first one, which actually predicts this plateau. However, as the higher harmonic terms would be less relevant than the fundamental, we can not conclude about the $m = 0$ plateau with this analysis. In fact, the zero-field problem needs a different approach, taking into account the O(3) symmetry of the model.[34] Second, the action (13) is the same as that obtained for spin-1/2 using bosonization,[19] but coming here from a large-S method. So, with the condition (14), we have

simply recovered the OYA result (3) on the possible values for magnetization plateaux to occur.

Finally, it is important to note that the factor of 3 in front of the Berry term $\frac{S-m}{a}\partial_\tau\phi_s$ is not an artifact of the transformation (11) and of the rescaling of the field. The rescaling is necessary for the following reason. As the $\vec{\varphi}$ fields are angular variable, they satisfy

$$\varphi_i(\tau=\beta)=\varphi_i(\tau=0)+2\pi n_i, \tag{16}$$

and the same condition for spatial periodic boundary conditions in $x=0$ and L. That gives similar conditions for the new fields $\vec{\phi}$, for instance, the antisymmetric combination ϕ_1 satisfies $\phi_1(\beta)=\phi_1(0)+2\pi(n_2-n_1)/\sqrt{2}$. But, given the form of the action S_{ch} for ϕ_1 and ϕ_2 (see below), we expect those fields to be small and therefore to have no winding, i.e, $n_1=n_2=0$. It remains for ϕ_s the periodicity $\phi_s(\beta)=\phi_s(0)+2\pi n_3/\sqrt{3}$. Thus, the rescaling $\phi_s\to\phi_s/\sqrt{3}$ is required to ensure a correct 2π periodicity.

3. *Chirality degree of freedom*

We now focus on the action S_{ch} for the fields ϕ_1 and ϕ_2, which stands for the chirality (nonmagnetic) degree of freedom we will introduce in Sec II C1. Before going into the technical details, a first comment is in order here. As we mentioned before, the chosen classical configuration on top of which the path-integral approach is constructed explicitly breaks the $\mathbb{Z}_2$ symmetry related to chirality. However, from the arguments shown below, we expect it to be able to reproduce almost all phases potentially observable for the spin tube.

It is convenient to introduce the two complex-conjugate fields $\Psi=\phi_1+i\phi_2$ and $\Psi^*=\phi_1-i\phi_2$ and, after rescaling the time, we get the action

$$S[\Psi,\Psi^*]=\int d\tau\,dx\left\{\frac{1}{2}K|\vec{\nabla}\Psi|^2+\tilde{M}^2|\Psi|^2 -2\mu(\Psi^*\partial_\tau\Psi-\Psi\partial_\tau\Psi^*)+\cdots\right\}, \tag{17}$$

where $K=\sqrt{\lambda_\tau^{(1,2)}\lambda_x^{(1,2)}}$ and $\tilde{M}^2=M^2\sqrt{\frac{\lambda_\tau^{(1,2)}}{\lambda_x^{(1,2)}}}$. We write $(\cdots)$ to remind that we are currently working in a second-order expansion and higher-order terms are expected in the general action. Although there is a mass term which is expected to open a gap, we argue in the following that the Berry term $\mu(\Psi^*\partial_\tau\Psi-\Psi\partial_\tau\Psi^*)$ may induce strong effects on the behavior of Ψ, namely, the possibility to have a gapless phase. We propose to treat qualitatively this question by using the symmetries to write a general action including important higher-order terms.

Going back to the initial fluctuation variables defined in Eq. (6), it is instructive to rewrite the field Ψ as $\Psi=i\frac{2}{\sqrt{6}}(\varphi_3+\omega\varphi_1+\omega^2\varphi_2)$, where $\omega=e^{i\frac{2\pi}{3}}$. So, under a circular permutation of the sites on a triangle, which leaves the system invariant, the field Ψ grabs a phase factor $\Psi\to\omega\Psi$. Then, the most general action invariant under such transformations has the form

$$S[\Psi,\Psi^*]=\int d\tau dx\left\{\frac{1}{2}K|\vec{\nabla}\Psi|^2-\mu(\Psi^*\partial_\tau\Psi-\Psi\partial_\tau\Psi^*) +\beta\Psi^3+\beta^*\Psi^{*3}+f(|\Psi|,\phi_s)+\cdots\right\}. \tag{18}$$

Writing $\Psi=\rho e^{i\theta}$, the only potentially gapless degree of freedom is the phase field θ, and the most general action reads as

$$S[\theta]=\int d\tau dx\left\{\frac{1}{2}\tilde{K}|\vec{\nabla}\theta|^2+\lambda_3\cos(3\theta)+\lambda_6\cos(6\theta) +i\mu\partial_\tau\theta\right\}, \tag{19}$$

where $\tilde{K}$, λ_3, λ_6, and μ are phenomenological parameters. The important point to note is that the original Berry phase causes the $i\mu\partial_\tau\theta$ term that forbid the vorticity (see the discussion for the symmetric action).

The effective action (19) tells us that there are four possible phases :

(i) When the stiffness $\tilde{K}$ of the field θ is large enough, the scaling dimensions $\delta_{3,6}\sim 1/\tilde{K}$ of the cosine terms are small and they are relevant so that $\langle\Psi\rangle\neq 0$. We first assume that λ_6 is negative. In this case, we have only three equivalent solutions for $\langle\Psi\rangle$ in which two of the three fields φ_i have the same value. To understand the consequences of this, let us go back to Eq. (9) and rewrite the penultimate term as $\Pi_1(\varphi_3-\varphi_2)+\Pi_2(\varphi_1-\varphi_3)+\Pi_3(\varphi_2-\varphi_1)\propto i(\Pi\Psi^*-\Pi^*\Psi)$, where the complex-conjugate fields Π and Π^* have the same definition as the fields Ψ,Ψ^* but with respect to the fluctuations Π_α. Having $\langle\Psi\rangle\neq 0$ implies $\langle\Pi\rangle\neq 0$, which translates into a homogeneous renormalization of the classical value of the magnetization. This correction is equal for two spins but different for the third one (note that the total magnetization is kept unchanged). We call this phase the symmetric spin imbalance.

(ii) The cosine operators are again relevant so that $\langle\Psi\rangle\neq 0$, but now λ_6 is positive. As for the phase (i), there is a homogeneous spin imbalance but with three different values for the magnetization, and we dub this phase an asymmetric spin-imbalance phase. The transition from the threefold degeneracy of the phase (i) to the sixfold degeneracy of this phase corresponds to the double sine-Gordon model, so it belongs to the universality class of the Ising transition.[37]

(iii) For a sufficiently small stiffness, the cosine operators become irrelevant. In that case, we perform a duality transformation as previously to take into account the role of the $i\partial_\tau\theta$ term. We end with two terms $(1/\tilde{K})(\vec{\nabla}\Theta)^2$ and $\lambda_2\cos[2\pi(\Theta+\eta x)]$, where Θ is the dual field of θ and η a phase modulation, *a priori* function of the microscopic parameters. For general η phases, the cosine is not commensurate and that eventually leads to a Gaussian model. This phase is characterized by $\langle\Psi\rangle=0$ and algebraic correlation functions for the θ field. We have a conformal field theory with central charge (see Sec. II D2) $c=1$.

(iv) $\langle\Psi\rangle=0$ and the correlation functions for the θ field are short ranged. Here, some comments are in order concerning the action (19). The last term, which originates from the Berry

phase, has the effect to suppress vortex configurations for the field θ and is responsible for the gapless phase (iii). It is also the same scenario found to explain that the field ϕ_s is gapless in general except for particular values of the magnetization. In the present case, as long as the parameter μ has a generic value, we said that the cosine operator of the dual field is forbidden.[38] Thus, the transition from the phase (iii) to this short-ranged phase should not be in principle via a Berezinsky-Kosterlitz-Thouless (BKT) transition. It would be rather because $\tilde{K} \to 0$, much in the same way as the XXZ chain enters into the ferromagnetic phase when the exchange anisotropy parameter becomes sufficiently negative. Such a ferrochiral phase has been found for $S = 1/2$ and weakly coupled chains in a wide range of the magnetic field by Sato in Ref. 28. He argued that this order should also survive when entering the plateau state for a moderately larger rung coupling.

C. Strongly coupled chains: Effective models and chirality

1. First-order perturbation Hamiltonians

In Sec. II B, we have discussed the model (2) regardless of the value of the spin S or the strength of the coupling parameters $J_\parallel$ and $J_\perp$. We eventually found a condition on the magnetization plateau values. In this section, we focus on the half-integer spin case and on the strong-coupling limit between the chains or weakly coupled triangles $J_\perp/J_\parallel \to \infty$. For a given half-integer S, we study the lowest and highest magnetization plateaux, namely, $m = 1/6$ and $m = S - 1/3$, as we will show they both can be described in terms of an additional chirality degree of freedom.

We start with the $S = 1/2$ case in the strong-coupling limit, and consider first the extreme case $J_\parallel = 0$ where the system is made of decoupled triangles. The ground state of a triangle is fourfold degenerate at $h = 0$, with two chiral spin-1/2 doublets. These states are

$$\begin{aligned}
|\uparrow L\rangle &= \frac{1}{\sqrt{3}}(|\uparrow\uparrow\downarrow\rangle + \omega|\uparrow\downarrow\uparrow\rangle + \omega^{-1}|\downarrow\uparrow\uparrow\rangle),\\
|\downarrow L\rangle &= \frac{1}{\sqrt{3}}(|\downarrow\downarrow\uparrow\rangle + \omega|\downarrow\uparrow\downarrow\rangle + \omega^{-1}|\uparrow\downarrow\downarrow\rangle),\\
|\uparrow R\rangle &= \frac{1}{\sqrt{3}}(|\uparrow\uparrow\downarrow\rangle + \omega^{-1}|\uparrow\downarrow\uparrow\rangle + \omega|\downarrow\uparrow\uparrow\rangle),\\
|\downarrow R\rangle &= \frac{1}{\sqrt{3}}(|\downarrow\downarrow\uparrow\rangle + \omega^{-1}|\downarrow\uparrow\downarrow\rangle + \omega|\uparrow\downarrow\downarrow\rangle),
\end{aligned} \tag{20}$$

where $\omega = e^{i\frac{2\pi}{3}}$. The indices L and R represent the chirality and $\uparrow$, $\downarrow$ the z-axis projection of the total spin of the triangle. It is important here to make the link with the field $\Psi \propto \varphi_3 + \omega\varphi_1 + \omega^2\varphi_2$ defined in the path-integral approach. Given the similar form of the states (20), it indicates clearly that the field Ψ (or equivalently the fields ϕ_1 and ϕ_2) describes this chirality degree of freedom. This is also consistent with the fact that the Berry phase of S_{ch} in Eq. (10) disappears in the opposite limit $J_\perp/J_\parallel \to 0$.

In this strong-coupling limit, we keep only the four states (20) to describe the low-energy physics around the zero magnetic field level crossing. To first order in $J_\parallel/J_\perp$, the effective Hamiltonian reads as

$$H_{\text{eff}} = \frac{J_\parallel}{3}\sum_j [1 + 4(\tau_j^+\tau_{j+1}^- + \tau_j^-\tau_{j+1}^+)]\vec{T}_j.\vec{T}_{j+1} - h\sum_j T_j^z, \tag{21}$$

where $\vec{T}_j$ is the triangle total spin-1/2 operator. We define the pseudo-spin-1/2 chirality operators $\tau_j^\pm$. They exchange chiralities L and R such as

$$\begin{aligned}
\tau^+|\cdot L\rangle = 0, \quad \tau^-|\cdot L\rangle = |\cdot R\rangle,\\
\tau^+|\cdot R\rangle = |\cdot L\rangle, \quad \tau^-|\cdot R\rangle = 0.
\end{aligned} \tag{22}$$

By construction, this effective Hamiltonian describes the system from zero magnetization up to the first plateau $m = 1/6$ with $\langle T_i^z\rangle = +1/2$, where only the two polarized states remain. This model has been studied both analytically and numerically.[13,23,26] Its spectrum displays a small plateau at magnetization $m = 0$, the spin gap arising from the dimerization of the ground state as explained in Sec. I. A strong enough magnetic field closes the gap and the system is then described by a two-component Luttinger liquid, with both spin and chirality modes being gapless.[26] Increasing again the magnetic field drives the system to the magnetization plateaux where only the two $T^z = +1/2$ states are present. The chirality is described by the XY Hamiltonian

$$H_{\text{eff}} = \frac{J_\parallel}{12}\sum_j [1 + 4(\tau_j^+\tau_{j+1}^- + \tau_j^-\tau_{j+1}^+)], \tag{23}$$

and is then critical.

This description remains valid for higher half-integer spins S. The low-energy space of one triangle at zero magnetic field is always spanned by two degenerate chiral doublets, the spin projections of which are $T^z = \pm 1/2$, so the above description used to derive the effective Hamiltonian can be repeated. The region from zero field up to the first plateau $m = 1/6$ is described by an Hamiltonian of the form (23), with only a change in the numerical constant of the chirality operators. On the plateau, the physical spin is frozen to $+1/2$ and the chirality is governed by an XY model, which reads as

$$H_{\text{eff}} = \frac{J_\parallel}{12}\sum_j [1 + \alpha(\tau_j^+\tau_{j+1}^- + \tau_j^-\tau_{j+1}^+)], \tag{24}$$

where the single parameter is $\alpha = (2S + 1)^2$.

Starting again from the decoupled case $J_\parallel = 0$, we observe that the above chirality description can also be used for the highest magnetization plateau $m = S - 1/3$, where the isolated triangle ground state is also twofold degenerate. Using again first-order perturbation theory, we find the chirality states on the plateau are also given in terms of an XY model of the same form as (24).

2. Range-2 CORE Hamiltonians

However, it turns out that these first-order effective Hamiltonians do not capture entirely the behavior of the chirality on these two extreme plateaux, as we observed numerically by measuring the central charges the existence of gapped phases for some range of the coupling (see Sec. II D2).

A way to go beyond the simple first-order perturbation theory is to use a contractor renormalization[39] (CORE)

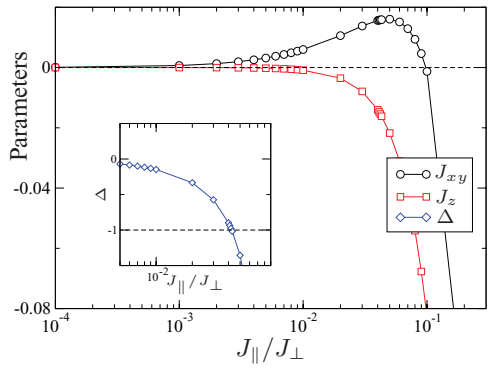

FIG. 3. (Color online) Values of the effective XXZ Hamiltonian parameters J_{xy}, J_z, and $\Delta = J_z/J_{xy}$ describing the chirality on the $m = 7/6$ plateau for a spin tube $S = 3/2$. The inset shows that at a critical coupling $J^h_{\parallel,c}/J_\perp = 0.042$, the chirality excitations become gapped and the model enters the ferrochiral phase.

approach to compute numerically an effective Hamiltonian. The CORE technique is a nonperturbative method of renormalization in real space for lattice systems used to build effective Hamiltonians reproducing the low-energy physics. It has been shown to give quantitative results, for instance, for various antiferromagnetic models,[40] including the presence of magnetic field.[41] Here, we truncate the calculation of the effective interactions to range 2, i.e., we consider only two coupled triangles. This is a quite simple computation, but it already gives a qualitative improvement over lowest-order perturbation since it produces an effective Hamiltonian of the XXZ type :

$$H_{\text{eff}} = \sum_j \left[\frac{J_{xy}}{2}(\tau_j^+\tau_{j+1}^- + \tau_j^-\tau_{j+1}^+) + J_z\tau_j^z\tau_{j+1}^z \right]. \quad (25)$$

We show in Fig. 3 the computed values of the parameters J_{xy}, J_z and their ratio $\Delta = J_z/J_{xy}$ governing the behavior of the model (25) for the plateau $m = 7/6$ in the case $S = 3/2$. For coupling values $J_\parallel/J_\perp < 0.042$, the system is in the regime $|\Delta| < 1$, the gapless XY phase with a central charge $c = 1$. As the coupling is increased, we see that the negative J_z component decreases and, at the critical value $J^h_{\parallel,c}/J_\perp = 0.042$, the system enters in the regime $\Delta < -1$, corresponding to the gapped ferromagnetic ("ferrochiral" here) phase with $c = 0$ (note that the central charge is rigorously defined only for a gapless critical phase) where all the triangles have the same chirality L or R. Note that the change of sign of J_{xy} does not change the nature of the phase as only the sign of J_z, which remains negative, is important. Also, we have checked by exact diagonalization (ED) for larger system lengths (up to $L = 10$) that there is a level crossing of the ground state close to this critical coupling, and its quantum numbers are compatible with the XY to ferrochiral scenario. Finally, the same scenario for Δ occurs for the lowest plateau $m = 1/6$ at a critical coupling $J^l_{\parallel,c}/J_\perp = 0.256$ (however, we will see with the DMRG results that for this value we are no longer in the plateau phase).

Even if this approach is straightforward, it allows us to explain qualitatively the possibility of a phase transition from a critical to a gapped phase. On the quantitative side, although longer-range effective interactions are expected to play a role (see below), the critical value $J^h_{\parallel,c}/J_\perp = 0.042$ found here is very close to the transition value observed with the DRMG.

TABLE I. Critical values $J^{\text{l}}_{\parallel,c}/J_\perp$ and $J^{\text{h}}_{\parallel,c}/J_\perp$ of the transition from an XY effective model to a ferromagnetic Ising one to describe the chirality behavior on the lowest and the highest magnetization plateaux (l and h superscripts, respectively).

	$S = 1/2$	$S = 3/2$	$S = 5/2$	$S = 7/2$	$S = 9/2$
$J^{\text{l}}_{\parallel,c}/J_\perp$	0.500	0.256	0.157	0.108	0.079
$J^{\text{h}}_{\parallel,c}/J_\perp$	0.500	0.0420	0.0140	0.0071	0.0042

As this nonperturbative CORE computation only involves solving two triangles, we can also treat higher spins. Table I shows, for different values of the half-integer spin S, the critical values $J^l_{\parallel,c}$ and $J^h_{\parallel,c}$ at which the chirality on the lowest and the highest plateaux is expected to undergo a quantum phase transition from the XY phase to the ferrochiral phase. For both plateaux, we observe that the gapless phase shrinks in the large-S limit. Again, the results given by this simple method are encouraging and we believe them to be actually quite accurate. Indeed, in the spin-1/2 case we find the value 0.500, very close to the value 0.496 computed with DMRG where the chirality enters the ferrochiral phase.[22] In the following, we will present DMRG data supporting these results for $S = 3/2$.

3. *General effective Hamiltonians*

Recently, Okunishi *et al.* have derived the second-order effective Hamiltonian in the spin-1/2 case,[22] which is a special case since it has only one plateau. New terms appear, such as a negative $\tau^z\tau^z$ one which can drive the system into an ordered phase. This is in agreement with the CORE calculation. Our goal is to propose an effective Hamiltonian capturing these phases and the transition. As the argument of the phase factor ω in Eq. (20) is nothing else than the transverse momentum, the effect of the operators $\tau^\pm$ is simply to shift the triangle momentum of $\pm 2\pi/3$. By transverse momentum conservation, the most general effective Hamiltonian, on both the first and last plateau, can be written as

$$H_{\text{eff}} = \sum_j \left[\frac{J_{xy}}{2}(\tau_j^+\tau_{j+1}^- + \tau_j^-\tau_{j+1}^+) + J_z\tau_j^z\tau_{j+1}^z + J_3(\tau_{j-1}^+\tau_j^+\tau_{j+1}^+ + \tau_{j-1}^-\tau_j^-\tau_{j+1}^-) + \cdots \right], \quad (26)$$

where we have dropped, for example, second-neighbor exchange terms. The values of the parameters of this model have been calculated up to second order in $J_\parallel/J_\perp$ (see Ref. 22). The $\tau^+\tau^+\tau^+$ term was obviously absent in our range-2 CORE calculation, but we would expect it to appear for a higher-range one. Notice that in this language, the $\mathbb{Z}_2$ symmetry associated with chirality is just $\tau^z \to -\tau^z$, which can be obtained for example with a rotation of π around the x axis. At this point, one can try to make connection with the results of the path integral. We have to keep in mind that, by construction, the $\mathbb{Z}_2$ chirality symmetry is broken within the path-integral approach. This corresponds to placing the effective spin

chain above at a nonzero average homogeneous magnetization $\langle \tau^z \rangle \neq 0$.

The bosonized form of this effective Hamiltonian was written recently in Ref. 22 as

$$H_{\text{eff}} = \frac{v}{2} \int dx \left[\frac{1}{2\kappa} (\partial_x \chi)^2 + 2\kappa (\partial_x \tilde{\chi})^2 + \lambda_1 \cos(2\sqrt{2\pi}\,\chi) + \lambda_2 \cos(6\sqrt{2\pi}\,\tilde{\chi}) \right], \quad (27)$$

where v is a Fermi velocity, κ is the Luttinger parameter, and $\tilde{\chi}$ is dual to χ. The second cosine operator is radiatively generated by the presence of the $\tau^+\tau^+\tau^+ +$ H.c. term. The first cosine operator is relevant for $\kappa < 1$, while the second becomes relevant for $\kappa > 9$. The gapless phase obtained between these two critical points is associated with the case (iii) predicted by the path integral in Sec. II B 3. For $J_\parallel/J_\perp \to 0$, the effective Hamiltonian (26) reduces to an XY model corresponding to $\kappa = 2$, thus both cosine terms are irrelevant and the chirality is in a critical phase. When the coupling ratio $J_\parallel/J_\perp$ is increased, it turns out that κ increases too as we are in the ferromagnetic regime, so the first cosine $\cos(2\sqrt{2\pi}\,\chi)$ will always be irrelevant.[42] We predict the gapless phase to disappear and two gapped phases should appear successively. The first one is caused by the $\cos(6\sqrt{2\pi}\,\tilde{\chi})$ term becoming relevant for some critical negative Δ_c, and the second corresponds to a transition to the ferrochiral phase when the magnitude of the negative Δ becomes sufficiently large. We associate this second phase to the case (iv) predicted by the path-integral approach. The first case eventually leads to the appearance of a gap in the chirality degrees of freedom in favor of a spin-imbalance phase similar to the one found in Ref. 22 but with one-step breaking of the translation symmetry.

Indeed, having a nonzero expectation value for the field $\tilde{\chi}$ makes the operator $\tau^x \sim (-1)^x \cos(\tilde{\chi})$ also nonzero. This corresponds to a symmetry breaking, as this operator is directly related to an imbalance in terms of the original spin operators.[43] As this phase is incompatible with a nonzero average magnetization in the z direction, it is inaccessible to the path-integral approach we have presented before. Also, the critical point at which the spin-imbalance phase would occur is expected to be very close to the regime in which the ferrochiral phase appears (which, in the absence of the three-body $\tau^+\tau^+\tau^+ +$ H.c. term, occurs for $\Delta = -1$). We then believe this phase to be only present in a very narrow range between the XY and the ferrochiral phases.

D. DMRG results for $S = 3/2$

1. Magnetization plateaux

In order to verify the previous predictions about the magnetization plateaux, which were established thanks to large-S techniques, we have performed numerical simulations using the DMRG algorithm[44] for $S = 3/2$ spin tubes with open boundary conditions (OBC) along the legs. We consider system lengths up to $L = 64$. Typically, we kept up to 2000 states and perform 20 sweeps, which is sufficient to have a discarded weight smaller than 10^{-8} or less.

In Fig. 4, we plot a typical magnetization curve obtained in the strongly coupled chains regime for $J_\parallel/J_\perp = 0.1$. Large

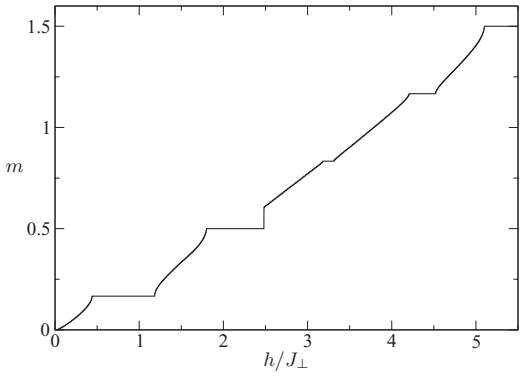

FIG. 4. Magnetization per spin curve (m) vs magnetic field h for the simple spin tube in the case $S = 3/2$. DMRG simulations were performed with $L = 64$ and $J_\parallel/J_\perp = 0.1$. Finite-size steps are almost not visible on this scale.

plateaux are observed below saturation for magnetization per site $m = 1/6$, $3/6$, $5/6$, and $7/6$, which correspond to the condition (14) that we have found with the field theory. Remember also that an $m = 0$ plateau was predicted, but it has a different nature (dimerization of the ground state), and on the scale of the figure, it is hardly visible.

In order to map out the phase diagram, we perform a finite-size analysis of the widths of each plateau for several couplings. Resulting data are shown in Fig. 5. While it confirms that all the plateaux found for $J_\parallel/J_\perp = 0.1$ are present in the thermodynamic limit, we do observe that each of them disappears for some different critical ratios of the coupling constants. These critical values of $J_\parallel/J_\perp$ are summarized in Table II along with the predicted values coming from the formula (15). It is important to mention that because the transitions between the plateau phases and the gapless phases are expected to be of the BKT type, it is difficult to locate them accurately. We also note that the predicted values are in a roughly good agreement with those coming from the DMRG. The main qualitative difference is that the path-integral approach predicts that the highest plateau, $m = 7/6$ here, should be the most robust. This prediction of the

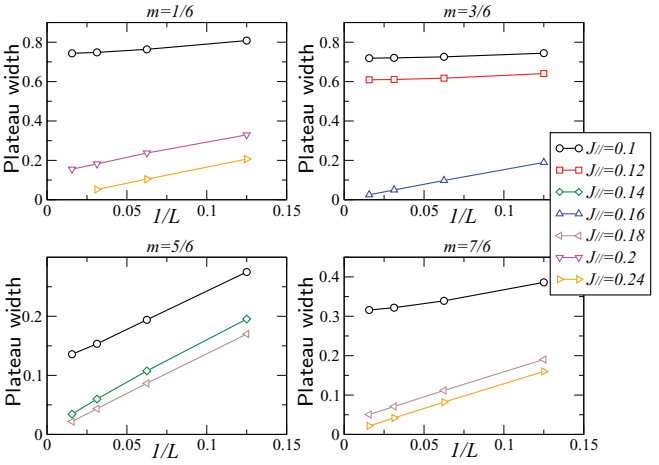

FIG. 5. (Color online) Finite-size scaling of the plateaux widths for different couplings $J_\parallel/J_\perp$.

TABLE II. Critical values $J_{\parallel,c}$ for the plateaux, in units of $J_\perp$, for the spin tube with $S = 3/2$. We indicate both the values found by DMRG and with the path integral (PI).

	$m = 1/6$	$m = 3/6$	$m = 5/6$	$m = 7/6$
$J_{\parallel,c}^{\mathrm{DMRG}}/J_\perp$	0.20–0.22	0.14–0.16	0.16–0.18	0.22–0.26
$J_{\parallel,c}^{\mathrm{PI}}/J_\perp$	0.066	0.074	0.098	0.19

plateaux disappearing gradually with m seems to be a general feature of the path-integral approach for chains or coupled chains. By performing extensive simulations, we arrive at the phase diagram shown in Fig. 6, where we indicate both the plateaux phases and the chirality phases discussed in the next section. It is clear that the predicted disappearance pattern for the plateaux is not recovered exactly, but we have to remember that the result (15) comes from a large-S approach. We plot the saturation field h_{sat}, which can be found analytically to be $h_{\mathrm{sat}} = (3J_\perp + 4J_\parallel)S$. We also indicate the existence of the $m = 0$ plateau, which we observe on the whole range of $J_\parallel/J_\perp$ but is not visible on this scale. For instance, we find the spin gap to be of order $2.10^{-2}J_\perp$ for $J_\parallel/J_\perp = 0.1$, a value in good agreement with other DMRG calculations.[30]

2. *Entanglement entropies and central charges*

Since the chirality degree of freedom has been shown to emerge for the extreme plateaux for half-integer spin, we now use large-scale DMRG simulations to investigate it. For $S = 1/2$, chirality is only expected on $m = 1/3$ plateau, and has already been confirmed numerically.[22] In our paper, we consider the next case, i.e., $S = 3/2$.

In order to check the existence of a chirality phase transition on the extreme plateaux, we simply compute the block von Neumann entropy $S_{vN}(\ell)$, which exhibits two different behaviors for large blocks ℓ and OBC: $S_{vN}(\ell)$ saturates to a constant when the system is fully gapped, whereas $S_{vN}(\ell) \simeq (c/6)\ln \ell$ where c is the central charge of the underlying conformal field theory.[45] In order to minimize

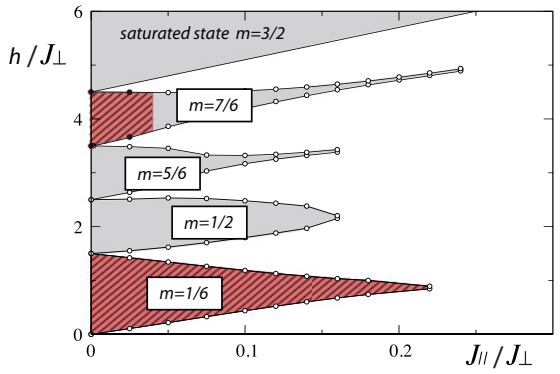

FIG. 6. (Color online) Phase diagram of the three-leg spin tube with $S = 3/2$ as a function of the coupling $J_\parallel$ and magnetic field h. Several magnetization plateaux can be observed (filled areas) and an additional $m = 0$ plateau is found (bold line). Data correspond to numerical simulations on 3×32 lattice with DMRG. Inside the extreme plateaux $m = 1/6$ and $7/6$, hashed red regions correspond to critical chirality phases (see Sec. II D2).

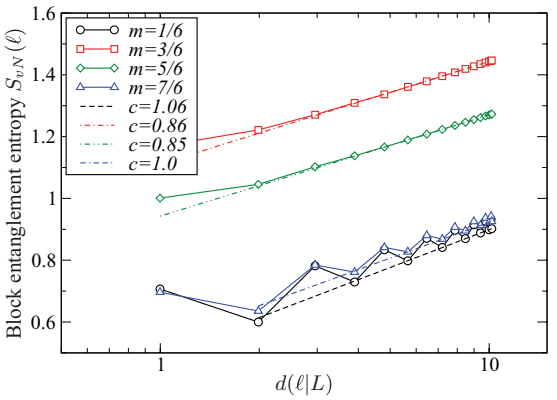

FIG. 7. (Color online) Block entropy $S_{vN}(\ell)$ vs block length $d(\ell|L)$ (starting at one end of the tube) for several magnetization plateaux on $L = 32$ spin tube. Coupling constants are fixed to $J_\parallel/J_\perp = 0.02$.

finite-size effects, we will consider the conformal block length $d(\ell|L) = (L/\pi)\sin(\ell\pi/L)$.

Guided by our CORE analysis, we first choose a small coupling $J_\parallel/J_\perp = 0.02$ where chirality is expected to be gapless on both $m = 1/6$ and $7/6$ plateaux. As it is shown in Fig. 7(a), numerical data are compatible with a gapless behavior with $c = 1$ in agreement with our expectation. We note that the intermediate plateaux $m = 3/6$ and $5/6$ also possess critical degrees of freedom, which could be compatible with $c = 1$ or a slightly smaller value. We plan to investigate in the future whether there could exist a non-Gaussian criticality nearby, or if it is simply due to numerical uncertainty when coupling constants have very different amplitudes. Anyway, for intermediate plateaux, there is no simple chirality language since more than two states per triangle (respectively four and three) are necessary to describe the low-energy configurations.

Now, we can increase the coupling constant $J_\parallel/J_\perp$ since the effective Hamiltonian and the CORE analysis indicate that the chirality degree of freedom should become gapped beyond some critical values (see Table I for $S = 3/2$). For instance, when fixing $J_\parallel/J_\perp = 0.1$, our data shown in Fig. 8 confirm that

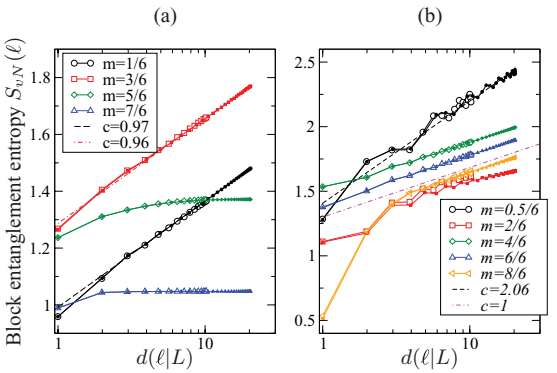

FIG. 8. (Color online) Block entropy $S_{vN}(\ell)$ vs block length $d(\ell|L)$ (starting at one end of the tube) for $L = 16$ (open symbols) and $L = 32$ (filled symbols). Coupling constants are fixed to $J_\parallel/J_\perp = 0.1$. (a) Magnetizations corresponding to plateaux; (b) intermediate magnetizations.

chirality has become gapped in the upper plateau, but remains gapless (with $c = 0.97$) for $m = 1/6$. The critical ratio that we find for gapless chirality on $m = 7/6$ plateau is close to 0.04, while chirality is always gapless on the $m = 1/6$ as long as it exists, i.e., for $J_\parallel/J_\perp \lesssim 0.25$. The quantum phase transition between gapless and gapped chirality phases for the upper plateau is indicated on the phase diagram (Fig. 6). The central result is that both critical values are in excellent agreement with our range-2 CORE estimates (see Table I).

For completeness, we also plot in Fig. 8(b) the scaling of the block entropy for intermediate magnetizations, which all correspond of course to critical gapless phases. In particular, at low magnetization, data are compatible with a two-component Luttinger liquid with $c = 2$ as predicted.[26] For all the other magnetizations, our data are compatible with a single gapless mode $c = 1$. It is beyond the scope of this work to study the interplay between chirality and magnetic degrees of freedom outside magnetization plateaux, but it could be interesting to investigate the stability of the ferrochiral phase for arbitrary magnetic field.[46]

3. Nature of the gapped phase

From the path-integral approach and the bosonization of the effective Hamiltonian, several different gapped phases are predicted to possibly occur when varying the coupling. However, the block entanglement entropies do not give any information about the nature of the gapped phase observed for $J_\parallel/J_\perp > 0.04$ in the upper $m = 7/6$ plateau. To investigate more precisely this question, we have computed the local magnetization values for different couplings, shown in Fig. 9.

In a very narrow range close to the phase transition, a clear *staggered* spin imbalance is observed in our simulations [see Fig. 9(a)], as predicted from the bosonized Hamiltonian (27). The local magnetizations vary around their mean value $m = 7/6$ with one chain having a clear different magnetization than the two others (in fact, we can not exclude the possibility that all three chains will have different magnetizations). While the symmetry can not be broken on a finite lattice, it turns out that DMRG simulations get locked in one of the degenerate ground states. Note also that the level crossing found by ED in this region could impede the accuracy of DMRG results here. It is interesting to contrast our result with the small *uniform* spin-imbalance phase found in the $S = 1/2$ tube, which seems to signal the entrance into a regime where the pseudo-spin-1/2 effective Hamiltonian is not valid anymore.[22]

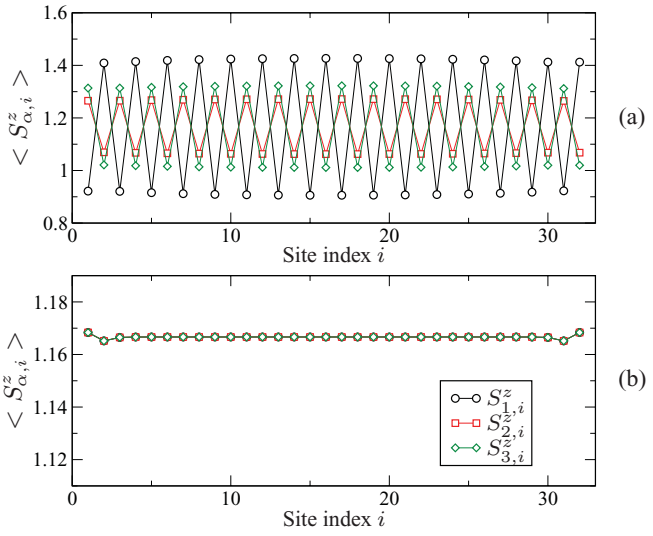

FIG. 9. (Color online) Local magnetizations obtained by DMRG simulations on a 3×32 spin tube with spin 3/2 on the $m = 7/6$ plateau. Upper and lower panels correspond, respectively, to (a) $J_\parallel/J_\perp = 0.04$ and (b) $J_\parallel/J_\perp = 0.06$.

When increasing slightly $J_\parallel/J_\perp$, but still deep in the plateau phase, we observe that all chains recover the same magnetization [see Fig. 9(b)], in agreement with having a ferrochiral phase.

In order to ascertain the validity of the description in terms of chiral degrees of freedom, as described in Sec. II C, we have computed by ED on a small 3×6 cluster with PBC the weights of these degrees of freedom in the reduced density matrix of one triangle (see Refs. 40 and 41 for a discussion of this technique). In a wide range of $J_\parallel/J_\perp \leqslant 0.08$ including the three different phases (XY, staggered spin imbalance, and ferrochiral), we find that the weights of these two states exceed 90%, so that we are rather confident that the effective model in terms of chirality remains valid.

III. TWISTED SPIN TUBE

A. The model and its experimental realization

Experimentally, only a few materials have been suggested to realize spin tube geometries. One such geometry, which we will study in this section, corresponds to the compound $[(CuCl_2tachH)_3Cl]Cl_2$. Magnetic measurements[47] have shown that it forms a twisted triangular spin tube. We call it "twisted" because of the different structure compared to the simple tube of Sec. II. The spins $S = 1/2$, coming from the copper ions, are arranged in a one-dimensional array of equilateral triangles, and each spin of a triangle is coupled to the spins of the two other chains of the neighboring triangles (Fig. 10). This corresponds to add diagonal couplings to the model (2) while the longitudinal one $J_\parallel$ vanishes. The Hamiltonian describing the twisted spin tube reads as

$$\begin{aligned} H &= H_\perp + H_d + H_h, \\ H_\perp &= J_\perp \sum_j \sum_{\alpha=1,2,3} \vec{S}_{\alpha,j} \cdot \vec{S}_{\alpha+1,j}, \\ H_d &= J_d \sum_j \sum_{\alpha=1,2,3} \vec{S}_{\alpha,j} \cdot (\vec{S}_{\alpha+1,j+1} + \vec{S}_{\alpha-1,j+1}), \\ H_h &= -h \sum_j \sum_{\alpha=1,2,3} S^z_{\alpha,j}, \end{aligned} \tag{28}$$

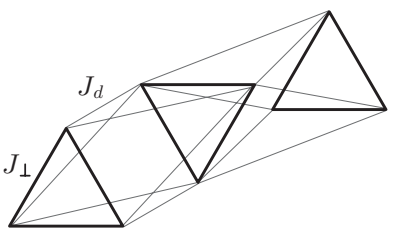

FIG. 10. Lattice structure of the twisted spin tube.

where J_d is the diagonal antiferromagnetic coupling. This model is believed to describe $[(CuCl_2tachH)_3Cl]Cl_2$ for the values $J_\perp = 0.9$ K and $J_d = 1.95$ K,[47], thus the compound belongs to neither the strong- nor weak-coupling regime. Theoretical and experimental investigations[48,49] have shown that this compound behaves essentially as a spin-3/2 chain, displaying a Luttinger liquid behavior.

B. Path-integral approach

Following the same steps as in Sec. II B, we start by finding the classical ground state of the Hamiltonian (28). Classically, the extreme cases $J_\perp = 0$ and $J_d = 0$ are easily understood in the absence of the magnetic field. For $J_\perp = 0$, the lattice is bipartite and the ground state is the Néel state. On the other hand, for $J_d = 0$, the triangles are decoupled and, as for the regular spin tube, the three spins are coplanar with a $2\pi/3$ angle between them. It turns out that the lowest-energy configuration is one of those two states in the whole range of the coupling parameters.[47] From $J_d/J_\perp = 0$ to $J_d/J_\perp = 3/2$, the ground state is the $2\pi/3$ state, and for higher values of $J_d/J_\perp$ it changes to the Néel state. This can be seen from a calculation in Fourier space by minimizing the resulting exchange coupling $J(k_\perp,k_\parallel) = 2\cos(k_\perp)[J_\perp + 2J_d\cos(k_\parallel)]$, where $k_\perp = 0,2\pi/3$. We have checked numerically that the effect of a magnetic field is just to polarize the spins in these two configurations and does not change the transition value $J_d/J_\perp = 3/2$. Thus, to investigate this model using the path-integral approach, we have to treat the two regimes separately.

1. Regime $J_d/J_\perp < 3/2$

In this range of $J_d/J_\perp$, all the triangles are in the same state, with angles of 120° between neighboring spins partially polarized by the magnetic field. This comes from the three-colorability of the lattice. This state is actually the same as the umbrella structure for the simple spin tube, but without the staggered order along the tube. We write this state as

$$\vec{S}_{\alpha,j} = S\begin{pmatrix} \sin(\theta_0)\cos\left(\varphi_\alpha^0\right) \\ \sin(\theta_0)\sin\left(\varphi_\alpha^0\right) \\ \cos(\theta_0) \end{pmatrix}, \tag{29}$$

where $\cos(\theta_0) = \frac{h}{S(3J_\perp+6J_d)}$ and $\varphi_\alpha^0 = (\alpha-1)2\pi/3$ up to an additional constant. Introducing the quantum fluctuations $\theta_0 \to \theta_{\alpha,j} = \theta_0 + \delta\theta_{\alpha,j}$, $\varphi_\alpha^0 \to \varphi_\alpha^0 + \varphi_{\alpha,j}$ and the conjugate momentum $\Pi_{\alpha,j}$, we get the same expansion (8) for the spin operators, except for the alternate order factor $(-1)^j$. Then, the action in the continuum limit reads as

$$\begin{aligned} S[\{\Pi_\alpha\},\{\varphi_\alpha\}] = \int d\tau\, dx \Bigg\{ & \sum_{\alpha=1,2,3}\left[\frac{1}{2}aJ_d(S^2-m^2)(\partial_x\varphi_\alpha)^2 + \frac{1}{2}a\frac{S^2}{S^2-m^2}(J_\perp+2J_d)\Pi_\alpha^2\right] \\ & + a\left(1-\frac{1}{2}\frac{m^2}{S^2-m^2}\right)(J_\perp+2J_d)(\Pi_1\Pi_2+\Pi_2\Pi_3+\Pi_3\Pi_1) \\ & + \frac{1}{4}\frac{S^2-m^2}{a}(J_\perp+2J_d)[(\varphi_1-\varphi_2)^2+(\varphi_2-\varphi_3)^2+(\varphi_3-\varphi_1)^2] \\ & - \frac{\sqrt{3}}{2}m(J_\perp+2J_d)\left[\Pi_1(\varphi_3-\varphi_2)+\Pi_2(\varphi_1-\varphi_3)+\Pi_3(\varphi_2-\varphi_1)\right] \\ & + i\sum_{\alpha=1,2,3}\left[\left(\frac{S-m}{a}\right)\partial_\tau\varphi_\alpha - \Pi_\alpha\partial_\tau\varphi_\alpha\right]\Bigg\}. \end{aligned} \tag{30}$$

This action has the same form as (9) for the simple tube, the only difference appearing in boundary terms. We observe that, except for the longitudinal part in $(\partial_x\varphi_\alpha)^2$, the couplings $J_\perp$ and J_d play the same role. More precisely, at large scale, one can argue that the diagonal coupling J_d is essentially identical to the perpendicular one. The factor of 2 for J_d simply tells that there are twice as many diagonal couplings as perpendicular per unit cell. Thus, we can follow the same steps and after performing the Gaussian integration, we find

$$\begin{aligned} S[\{\phi_\alpha\}] &= S_{ch}[\phi_1,\phi_2] + S_s[\phi_s], \\ S_{ch}[\phi_1,\phi_2] &= \int d\tau\, dx\left\{\frac{1}{2}\lambda_\tau^{(1,2)}[(\partial_\tau\phi_1)^2+(\partial_\tau\phi_2)^2] + \frac{1}{2}\lambda_x^{(1,2)}[(\partial_x\phi_1)^2+(\partial_x\phi_2)^2] - i\mu(\phi_1\partial_\tau\phi_2-\phi_2\partial_\tau\phi_1)\right\}, \\ S_s[\phi_s] &= \int d\tau\, dx\left\{\frac{1}{2}\lambda_\tau^{(s)}(\partial_\tau\phi_s)^2 + \frac{1}{2}\lambda_x^{(s)}(\partial_x\phi_s)^2 + i3\frac{S-m}{a}\partial_\tau\phi_s\right\}, \end{aligned} \tag{31}$$

where the constants are functions of the microscopic parameters.

At this order, the action is again decoupled into a symmetric action for ϕ_s and a chirality action for the two other fields ϕ_1 and ϕ_2. Surprisingly, the mass of the latter vanishes after momentum Π_α integration. However, it does not invalidate our previous discussion about the necessary rescaling of ϕ_s. Indeed, the expansion (8) for the spin operators and for the Hamiltonian is restricted to second order in the fields. Expanding up to fourth order, mass terms in $(\varphi_\alpha - \varphi_{\alpha+1})^4$

would appear and we would recover a mass term, ensuring that ϕ_1 and ϕ_2 are still small. Apart from this mass cancellation, there is no difference with the simple spin tube case. This is expected as they both have the same classical configuration in this regime of $J_d/J_\perp$. For the twisted tube, the staggered order is in the diagonal coupling, as the angle between spins coupled by J_d is larger than $\pi/2$.

Then, we perform the duality transformation on the symmetric part of the action. We obtain the plateaux existence condition $3(S-m) \in \mathbb{Z}$, which is obviously the same as for the simple tube since it does not depend on the detailed geometry but only on the unit cell. We also compute the expression of the cosine operator dimension

$$\delta = \pi \sqrt{\frac{3J_d(S^2-m^2)}{J_\perp\left(1+2\frac{J_d}{J_\perp}\right)}}, \tag{32}$$

which is very similar to the simple tube case (15) and bears the same functional form with m. From the dependence on the microscopic parameters, we predict again to observe plateau in the strong-coupling regime along the rungs.

Concerning the fields ϕ_1 and ϕ_2, they describe the chirality degrees of freedom as for the simple spin tube. The form of the action being the same, the same reasoning as in Sec. II B3 holds and the same four phases are possible. Particularly, we claim again that the Berry term in this action makes possible a chiral gapless phase for some values of the microscopic parameters we are not able to compute (but still *a priori* in the strong-coupling regime). Moreover, we expect that in the present case, there are more chances to be in this phase compared to the simple tube case because of the vanishing bare mass.

2. Regime $J_d/J_\perp > 3/2$

We start here from the partially polarized Néel state, parametrized as

$$\vec{S}_{\alpha,j} = S\begin{pmatrix}(-1)^j\sin(\theta_0)\cos(\varphi_0)\\(-1)^j\sin(\theta_0)\sin(\varphi_0)\\\cos(\theta_0)\end{pmatrix}, \tag{33}$$

where $\cos(\theta_0) = h/(8SJ_d)$ and we choose $\varphi_0 = 0$, this freedom of choice reflecting the U(1) degeneracy of the ground state.

Then, we proceed as usual, allowing these angles to fluctuate by small quantities $\delta\theta_{\alpha,j}$ and $\varphi_{\alpha,j}$ as $\theta_0 \to \theta_{\alpha,j} = \theta_0 + \delta\theta_{\alpha,j}$, $\varphi_\alpha^0 \to \varphi_{\alpha,j}$, and introducing new variables $\Pi_{\alpha,j}$ conjugates of the $\varphi_{\alpha,j}$'s. Following the same steps as previously, namely, rewriting the Hamiltonian as a function of these fluctuation variables, expanding up to second order in the fields, and taking the continuum limit, we obtain the action

$$\begin{aligned}S[\{\Pi_\alpha\},\{\varphi_\alpha\}] = \int d\tau\, dx \Bigg\{ &\sum_{\alpha=1,2,3}\left[aJ_d(S^2-m^2)(\partial_x\varphi_\alpha)^2 + a(2J_d-J_\perp)\frac{S^2}{S^2-m^2}\Pi_\alpha^2\right]\\ &+\frac{1}{2}(2J_d-J_\perp)\frac{S^2-m^2}{a}[(\varphi_1-\varphi_2)^2+(\varphi_2-\varphi_3)^2+(\varphi_3-\varphi_1)^2]\\ &+a\left[2J_d\left(1-\frac{m^2}{S^2-m^2}\right)+J_\perp\frac{S^2}{S^2-m^2}\right](\Pi_1\Pi_2+\Pi_2\Pi_3+\Pi_3\Pi_1)\\ &+i\sum_{\alpha=1,2,3}\left[\left(\frac{S-m}{a}\right)\partial_\tau\varphi_\alpha - \Pi_\alpha\partial_\tau\varphi_\alpha\right]\Bigg\}.\end{aligned} \tag{34}$$

The condition $2J_d > J_\perp$ for the action to be positive-definite is automatically fulfilled as we started from the assumption $J_d/J_\perp > 3/2$. The collinear nature of the classical ground state is reflected in the absence of the terms $\Pi_\alpha(\varphi_{\alpha+1}-\varphi_{\alpha-1})$ [see Eqs. (9) or (30)].

The next steps are to use again the transformation (11), perform the Gaussian integration in the Π_α fields, and rescale the symmetric field as $\phi_s \to \phi_s/\sqrt{3}$. This leads to the action

$$\begin{aligned}S[\{\phi_\alpha\}] &= S_{ch}[\phi_1,\phi_2] + S_s[\phi_s],\\ S[\{\phi_\alpha\}] &= \int d\tau\, dx\left\{\frac{1}{2}\lambda_\tau^{(1,2)}[(\partial_\tau\phi_1)^2+(\partial_\tau\phi_2)^2] + \frac{1}{2}\lambda_x^{(1,2)}[(\partial_x\phi_1)^2+(\partial_x\phi_2)^2] + M^2\left(\phi_1^2+\phi_2^2\right)\right\},\\ S_s[\phi_s] &= \int d\tau\, dx\left\{\frac{1}{2}\lambda_\tau^{(s)}(\partial_\tau\phi_s)^2 + \frac{1}{2}\lambda_x^{(s)}(\partial_x\phi_s)^2 + i3\frac{S-m}{a}\partial_\tau\phi_s\right\}.\end{aligned} \tag{35}$$

Although we end with the same decoupling as previously, this action is actually quite different than Eqs. (10) and (31). The crucial point is that there is no Berry term $i(\phi_1\partial_\tau\phi_2 - \phi_2\partial_\tau\phi_1)$ here. Thus, those fields are automatically gapped, and there is no possibility of either an emergent gapless phase or a spin-imbalance phase [no $i(\Pi\Psi^* - \Pi^*\Psi)$ term], contrary to the regime $J_d/J_\perp < 3/2$ or for the simple tube. This is not surprising, however, given the fact that we are not in the strong-coupling regime and so there is no possibility for the chirality described by those two fields to be gapless (or more

explicitly, there is no chirality in a collinear configuration). Then, they only correspond to high-energy excitations and we can integrate them out by using the saddle-point solution $\phi_1 = \phi_2 = 0$.

It remains only the action for the symmetric field, which is exactly the same we have already encountered. We apply the duality transformation and repeat our analysis of the dual action. At the end, we recover the plateaux condition $3(S - m) \in \mathbb{Z}$. On the other hand, the situation is very different for the scaling dimension, as we find it to be independent of the parameters of the microscopic model in this second-order calculation. It reads as

$$\delta = \frac{3}{2}\pi\sqrt{S^2 - m^2}\,. \tag{36}$$

This means that a plateau will either be always present or always absent when $J_d/J_\perp > 3/2$. More precisely, if a plateau is absent for a given spin value, then it will also be absent for higher spins.

3. Discussion

Using the results derived above, we are able to discuss the case of $[(CuCl_2tachH)_3Cl]Cl_2$, which belongs to the $J_d/J_\perp > 3/2$ regime. For $S = 1/2$, the OYA condition predicts only one plateau at a magnetization per spin $m = 1/6$, or $1/3$ of the saturation value. The scaling dimension is $\delta = \pi/\sqrt{2} > 2$ for these values, so the cosine operator is irrelevant. With this result, we predict that the compound does not possess any plateau in its magnetization curve. In a previous work, Fouet *et al.*[48] reached the same conclusion. They found that for the realistic coupling values $J_d/J_\perp = 2.16$, the model (28) behaves as an effective spin-3/2 antiferromagnetic chain with no plateau, and their DMRG calculations confirmed this effective Hamiltonian approach.

Overall, our analysis is consistent with their numerical phase diagram based on the DMRG. Indeed, they observed a finite size for the $m = 1/6$ plateau from $J_d/J_\perp = 0$ to about $J_d/J_\perp = 3/2$, where it vanishes. We find here the same result. Although the form of the action of the symmetric field is the same starting either from the $2\pi/3$ state for $J_d/J_\perp < 3/2$ or from the collinear Néel state for $J_d/J_\perp > 3/2$, the scaling dimension of the cosine term indicates that in the first case the plateau is always present, while it disappears in the second one. In consequence, we expect qualitatively the same phase diagram with two different regimes. However, we should consider carefully this result, as for higher spin $S = 3/2$, DMRG calculations seem to indicate that the plateau $m = 3/6$ vanishes also at $J_d/J_\perp = 3/2$, or very close to this point (see below). Thus, the important point is that we have obtained two different results for the scaling dimension of the cosine term. One is that it is independent of the microscopic parameters. The other is that is is dependent on the value $J_d/J_\perp$, which tells us that we could observe plateaux. But, we should keep in mind that the critical values predicted come from a large-S analysis.

C. Strongly coupled chains

The triangular unit cell being the same as in the simple tube case, the same procedure as done in Sec. II C can be applied to build an effective Hamiltonian on the lowest and the highest magnetization plateaux. For instance, the effective Hamiltonian to first-order perturbation in $J_d/J_\perp$ for the spin-1/2 twisted spin tube on the unique $m = 1/6$ plateau reads as[48]

$$H_{\text{eff}} = \frac{J_d}{6}\sum_j [1 + 2(\tau_j^+\tau_{j+1}^- + \tau_j^-\tau_{j+1}^+)], \tag{37}$$

where the chirality operator τ is defined in Eq. (22). Thus, to go beyond this perturbation theory, we propose the same form (26) for general Hamiltonians describing the emerging chirality degrees of freedom along with its bosonized form (27). It follows that the same succession of a gapless phase then two gapped phases is predicted, as for the simple tube.

Keeping only the XXZ part of Eq. (26), we use again a range-2 CORE calculation as in Sec. II C2 to extract numerical values for J_{xy} and J_z. Surprisingly, at this level of approximation, we find a completely different result compared to the simple tube case, namely, the absence of the XY-ferrochiral transition. For the twisted tube, the chirality remains in the $|\Delta| < 1$ phase on both plateaux as the coupling $J_\parallel$ increases. Moreover, we also find this absence of a gapped phase for higher half-integer spins, contrary to the simple tube study which shows the disappearance of the XY phase in the large-S limit. From this CORE calculation, we do not find a gapped phase.

D. DMRG results for $S = 3/2$

We now consider the $S = 3/2$ case using large-scale numerical simulations with DMRG algorithm (details are identical to Sec. II D). First, we confirm that magnetization plateaux that satisfy OYA criterion $3(S - m) \in \mathbb{Z}$ exist for small intertriangle coupling, such as $J_d/J_\perp = 0.1$ as shown in Fig. 11.

By performing a finite-size analysis of the plateaux widths, we can obtain the phase diagram in magnetic field, shown in Fig. 12. As for the simple tube, the precise location of the plateau regions can be quite hard due to BKT transitions. In the plot, we have used as a simple criterion that the extrapolated plateau should be larger than $0.005J_\perp$ to be considered as

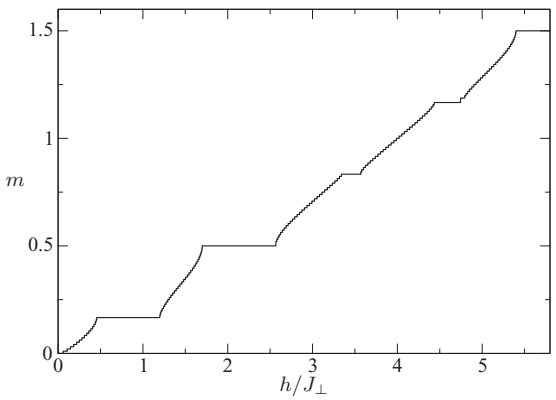

FIG. 11. Magnetization curve (m) vs magnetic field h for the twisted three-leg spin tube in the case $S = 3/2$. DMRG simulations were performed with $L = 32$ and $J_d/J_\perp = 0.1$.

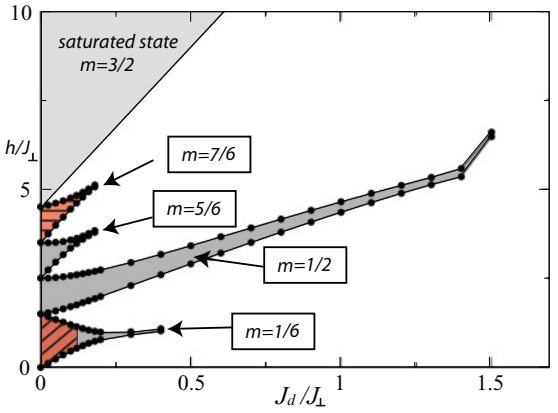

FIG. 12. (Color online) Phase diagram of the twisted spin tube with $S = 3/2$ as a function of the couplings J_d and magnetic field h. Several magnetization plateaux can be observed (filled regions) and an additional $m = 0$ plateau is also found (but is much smaller and not shown on the figure). Data correspond to numerical simulations on 3×32 lattice with DMRG. Red hashed areas correspond to critical chirality regions (see text).

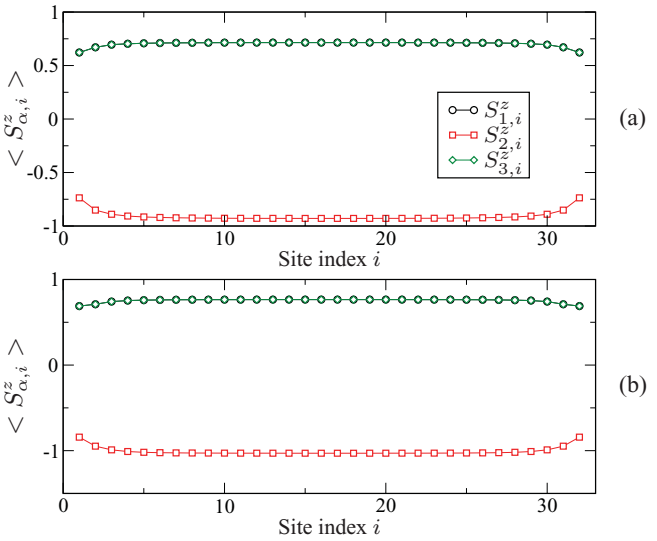

FIG. 13. (Color online) Local magnetizations obtained by DMRG simulations on a 3×32 twisted spin tube with spin $3/2$ on the $m = 1/6$ plateau. Upper and lower panels correspond, respectively, to (a) $J_d/J_\perp = 0.2$ and (b) $J_d/J_\perp = 0.3$.

finite. Similarly to Fig. 6, there also exists a plateau at $m = 0$, which corresponds to a spontaneous dimerization of the tube and is not the subject of our present study. We find that the largest plateau corresponds to $m = 1/3$ and is stable in all the region $J_d/J_\perp \leqslant 3/2$; it exhibits a small anomaly at the tip, similar to what is found in the $S = 1/2$ case.[48] For a given $J_d/J_\perp$ and increasing h, we also note that the order of disappearance of the plateaux disagrees with the path-integral prediction, as in the simple tube case. This may be due to renormalization effects in the field-theory parameters since the field theory is valid at large S and we are considering $S = 3/2$ here.

Following Sec. II D2, we now turn to the investigation of the chirality for the extreme plateaux $m = 1/6$ and $7/6$. According to the range-2 CORE Hamiltonian of the previous section, we expect to observe criticality for these degrees of freedom in all the plateaux. Computing the scaling of the block entanglement entropy with DMRG (data not shown), we observe that while it seems to be the case for $m = 7/6$, we do find a transition to a fully gapped regime in the lower plateau $m = 1/6$ when $J_d/J_\perp = 0.12$ (red hashed regions in Fig. 12). But, it turns out that the mechanism gapping the chirality is here very different from the scenario determined for the simple tube. Computing the local magnetizations for the three chains, we find neither a staggered spin-imbalance phase nor a ferrochiral phase. Instead, we find for $J_d/J_\perp > 0.12$ a unique *uniform* spin imbalance following the critical phase. The imbalance is very strong as shown in Fig. 13, one chain having a negative magnetization, and it holds up until the disappearance of the plateau.

The explanation for the absence of the two gapped phases present in the strong-coupling limit is given by the reduced density-matrix weights. In contrast to the simple tube case, the weights of the two chiral states rapidly become quite small (for instance, 47% for a 3×6 twisted tube with $J_d/J_\perp = 0.3$ as found by ED). Thus, for such values, we can not rely on the effective Hamiltonian. Note that a similar argument involving a mixing with other triangle states, thus prohibiting the use of the effective model, was given in Ref. 22 to explain the uniform spin imbalance phase found for the simple $S = 1/2$ spin tube at magnetization $m = 1/3$. Instead, we have to rely on the path-integral results, valid for any $J_d/J_\perp$, which indeed predict this uniform spin-imbalance phase. The important remark here is that, despite the important difference between the two tubes, we are able to understand all the phases observed by combining the results of the path integral and of the bosonized form of the strong-coupling Hamiltonian.

IV. CONCLUSION

In this paper, we have studied the magnetic and nonmagnetic properties of frustrated three-leg spin tubes under a magnetic field. We have considered two kinds of geometries, one of which is relevant for the recently studied compound $[(CuCl_2tachH)_3Cl]Cl_2$. Our first result concerns the presence of plateaux in the magnetization curve. We give the values of the magnetization at which such plateaux can appear given the magnitude S of the spins, as well as the critical couplings for which such plateaux are expected to appear. We have used two complementary techniques. The first one is the path-integral method, which, because of the topological nature of the Berry phase term, gives trustable qualitative results for any value of S, and whose prediction of critical couplings are expected to be also quantitatively accurate for large S. The second technique used is the DMRG method, which is, however, more suited to relatively small spins S.

While magnetization plateaux are not specific to frustrated systems, there are emergent low-energy degrees of freedom, the presence of which are due to frustration. For historical reasons, we have dubbed those degrees of freedom chirality degrees of freedom. Their origin comes from degeneracies in the ground state for decoupled triangles, which motivates the use of a third technique to complement the path integral

and DMRG. This strong-coupling technique corresponds to studying an effective Hamiltonian in a reduced Hilbert space where high-energy degrees of freedom are neglected. This supplementary degree of freedom can remain gapless even when the magnetization degrees of freedom are gapped (in the magnetization plateau). Here again, the agreement between the three techniques for predicting the critical couplings at which such degrees of freedom disappear is qualitatively excellent and quantitatively quite satisfactory. It is important to stress that, although we restricted ourselves to the cases of two degenerate spin-1/2 representations for half-integer spin cases, the chirality is in principle a generic feature that can give rise to more complicated effective Hamiltonians. It could arise also for integer spin tubes, provided they are tuned to the appropriate value of the magnetization.

With the results obtained here and the excellent complementarity of the path-integral technique, the effective Hamiltonian approach and the DMRG calculations are very encouraging. Indeed, the study of potentially gapless nonmagnetic degrees of freedom has become a central topic in the study of exotic phases in frustrated quantum magnetism. In the systems analyzed here, one important generalization that deserves futures studies is the interplay of doping with such degrees of freedom. It is by now relatively well established that doping will result in shifts and splitting of the magnetization plateaux in such quasi-one-dimensional systems,[50–52] but how doping may affect the nonmagnetic degrees of freedom is still an open problem. The other important extension concerns the role of such nonmagnetic degrees of freedom in higher-dimensional frustrated systems, where some results for distorted kagome lattices are indeed quite instructive.[53,54] A chirality also appears for instance in the study of trimerized Mott insulators.[55] The emergence of new analytical and numerical techniques for studying such issue in two- and three-dimensional frustrated magnets are also very promising.

ACKNOWLEDGMENTS

We would like to thank P. Lecheminant, E. Orignac, and K. Totsuka for enlightening discussions. Numerical simulations were performed using HPC resources from GENCI-IDRIS (Grant No. 2012050225) and CALMIP.

APPENDIX: DUALITY TRANSFORMATION

We present here the details of the duality transformation used on the symmetric part S_s of the action (10). First, we perform a Hubbard-Stratonovich transformation introducing an auxiliary field $\vec{J} = (J_\tau, J_x)$ and we divide the field ϕ_s in two parts $\phi_s = \phi_{s,v} + \phi_{s,f}$, where $\phi_{s,f}$ has no vorticity $(\partial_\mu\partial_\nu - \partial_\nu\partial_\mu)\phi_{s,f} = 0$. The action reads as

$$S[\phi_{s,v},\phi_{s,f},\vec{J}] = \int d\tau\, dx \Big\{ \frac{1}{2\lambda_\tau^{(s)}} J_\tau^2 + \frac{1}{2\lambda_x^{(s)}} J_x^2 + i\left(J_\tau + 3\frac{S-m}{a}\right)\partial_\tau\phi_{s,v} + i J_x \partial_x \phi_{s,v} + i\left(J_\tau + 3\frac{S-m}{a}\right)\partial_\tau\phi_{s,f} + i J_x \partial_x \phi_{s,f} \Big\}. \tag{A1}$$

Integrating by parts the last two terms containing the vorticity-free component, the action takes the form

$$S[\phi_{s,v},\phi_{s,f},\tilde{\vec{J}}] = \int d\tau dx \Big\{ \frac{1}{2\lambda_\tau^{(s)}}\left(\tilde{J}_\tau - 3\frac{S-m}{a}\right)^2 + \frac{1}{2\lambda_x^{(s)}}\tilde{J}_x^2 + i(\tilde{J}_\tau\partial_\tau + \tilde{J}_x\partial_x)\phi_{s,v} - i(\partial_\tau\tilde{J}_\tau + \partial_x\tilde{J}_x)\phi_{s,f} \Big\}, \tag{A2}$$

where we have defined $\tilde{\vec{J}} = (J_\tau + 3\frac{S-m}{a}, J_x)$. The vorticity-free part simply leads to a zero divergence constraint on the auxiliary field $\partial_\tau\tilde{J}_\tau + \partial_x\tilde{J}_x = 0$ and we obtain

$$S[\phi_{s,v},\tilde{\vec{J}}] = \int d\tau\, dx \Big\{ \frac{1}{2\lambda_\tau^{(s)}}\left(\tilde{J}_\tau - 3\frac{S-m}{a}\right)^2 + \frac{1}{2\lambda_x^{(s)}}\tilde{J}_x^2 + i\tilde{J}_\mu\partial_\mu\phi_{s,v} \Big\}. \tag{A3}$$

The constraint can be solved in one dimension by introducing the dual field Φ_s defined by $\tilde{J}_\mu = \epsilon_{\mu\nu}\partial_\nu\Phi_s$, this field being vorticity free. Then, we integrate by parts the last term in Eq. (A3) and, with the redefinition $\tilde{\Phi}_s = \Phi_s - 3\frac{S-m}{a}x$, we get

$$S[\tilde{\Phi}_s] = \int d\tau\, dx \Big\{ \frac{1}{2\lambda_x^{(s)}}(\partial_\tau\tilde{\Phi}_s)^2 + \frac{1}{2\lambda_\tau^{(s)}}(\partial_x\tilde{\Phi}_s)^2 + i2\pi\rho_v\left(\tilde{\Phi}_s + 3\frac{S-m}{a}x\right) \Big\}. \tag{A4}$$

In this action, ρ_v is the space-time density of vortices defined as $(\partial_\tau\partial_x - \partial_x\partial_\tau)\phi_v = \epsilon_{\mu\nu}\partial_\mu\partial_\nu\phi_v = 2\pi\sum_j q_{j,v}\delta(\tau - \tau_{j,v})\delta(x - x_{j,v}) = 2\pi\rho_v$ with $(\tau_{j,v}, x_{j,v})$ the space-time coordinates of the jth vortex and $q_{j,v} \in \mathbb{Z}$ its charge. After summing over all the vortex configurations in the partition function and rescaling the imaginary time, we finally end with the action

$$S[\tilde{\Phi}_s] = \int d\tau\, dx \Big\{ \frac{1}{2}K(\vec{\nabla}\tilde{\Phi}_s)^2 + g_1\cos\left(2\pi\left[\tilde{\Phi}_s + 3\frac{S-m}{a}x\right]\right) \Big\}, \tag{A5}$$

where $K = 1/\sqrt{\lambda_\tau^{(s)}\lambda_x^{(s)}}$, $\vec{\nabla} = (\partial_\tau, \partial_x)$, and g_1 is a constant we have not calculated.

[1] E. Dagotto and T. M. Rice, Science **271**, 618 (1996).
[2] H. J. Schulz, Phys. Rev. B **34**, 6372 (1986).
[3] S. R. White, R. M. Noack, and D. J. Scalapino, Phys. Rev. Lett. **73**, 886 (1994).
[4] D. Sénéchal, Phys. Rev. B **52**, 15319 (1995).

[5]D. C. Cabra, A. Honecker, and P. Pujol, Phys. Rev. Lett. **79**, 5126 (1997).
[6]D. C. Cabra, A. Honecker, and P. Pujol, Phys. Rev. B **58**, 6241 (1998).
[7]K. Kojima, A. Keren, G. M. Luke, B. Nachumi, W. D. Wu, Y. J. Uemura, M. Azuma, and M. Takano, Phys. Rev. Lett. **74**, 2812 (1995).
[8]R. S. Eccleston, T. Barnes, J. Brody, and J. W. Johnson, Phys. Rev. Lett. **73**, 2626 (1994).
[9]F. D. M. Haldane, Phys. Rev. Lett. **50**, 1153 (1983).
[10]S. P. Strong and A. J. Millis, Phys. Rev. Lett. **69**, 2419 (1992).
[11]M. Azuma, Z. Hiroi, M. Takano, K. Ishida, and Y. Kitaoka, Phys. Rev. Lett. **73**, 3463 (1994).
[12]G. Chaboussant, P. A. Crowell, L. P. Lévy, O. Piovesana, A. Madouri, and D. Mailly, Phys. Rev. B **55**, 3046 (1997).
[13]K. Kawano and M. Takahashi, J. Phys. Soc. Jpn. **66**, 4001 (1997).
[14]T. Sakai, M. Sato, K. Okamoto, K. Okunishi, and C. Itoi, J. Phys.: Condens. Matter **22**, 403201 (2010).
[15]Y. Narumi, M. Hagiwara, R. Sato, K. Kindo, H. Nakano, and M. Takahashi, Phys. B: Condens. Matter **246-247**, 509 (1998).
[16]W. Shiramura, K. ichi Takatsu, B. Kurniawan, H. Tanaka, H. Uekusa, Y. Ohashi, K. Takizawa, H. Mitamura, and T. Goto, J. Phys. Soc. Jpn. **67**, 1548 (1998).
[17]Y. Yoshida, O. Wada, Y. Inagaki, T. Asano, K. Takeo, T. Kawae, K. Takeda, and Y. Ajiro, J. Phys. Soc. Jpn. **74**, 2917 (2005).
[18]H. Kikuchi, Y. Fujii, M. Chiba, S. Mitsudo, T. Idehara, T. Tonegawa, K. Okamoto, T. Sakai, T. Kuwai, and H. Ohta, Phys. Rev. Lett. **94**, 227201 (2005).
[19]M. Oshikawa, M. Yamanaka, and I. Affleck, Phys. Rev. Lett. **78**, 1984 (1997).
[20]E. Lieb, T. Schultz, and D. Mattis, Ann. Phys. (NY) **16**, 407 (1961).
[21]A. Tanaka, K. Totsuka, and X. Hu, Phys. Rev. B **79**, 064412 (2009).
[22]K. Okunishi, M. Sato, T. Sakai, K. Okamoto, and C. Itoi, Phys. Rev. B **85**, 054416 (2012).
[23]H. Schulz, in *Strongly Correlated Magnetic and Superconducting Systems*, Lecture Notes in Physics, Vol. 478, edited by G. Sierra and M. Martn-Delgado (Springer, Berlin, 1997), p. 136.
[24]T. Sakai, M. Sato, K. Okunishi, Y. Otsuka, K. Okamoto, and C. Itoi, Phys. Rev. B **78**, 184415 (2008).
[25]K. Tandon, S. Lal, S. K. Pati, S. Ramasesha, and D. Sen, Phys. Rev. B **59**, 396 (1999).
[26]E. Orignac, R. Citro, and N. Andrei, Phys. Rev. B **61**, 11533 (2000).
[27]R. Citro, E. Orignac, N. Andrei, C. Itoi, and S. Qin, J. Phys.: Condens. Matter **12**, 3041 (2000).
[28]M. Sato, Phys. Rev. B **75**, 174407 (2007).
[29]M. Sato and T. Sakai, Phys. Rev. B **75**, 014411 (2007).
[30]S. Nishimoto, Y. Fuji, and Y. Ohta, Phys. Rev. B **83**, 224425 (2011).
[31]M. Sato, Phys. Rev. B **72**, 104438 (2005).
[32]M. Sato, J. Phys. Chem. Solids **66**, 1454 (2005).
[33]M. Sato and M. Oshikawa, Phys. Rev. B **75**, 014404 (2007).
[34]D. Charrier, S. Capponi, M. Oshikawa, and P. Pujol, Phys. Rev. B **82**, 075108 (2010).
[35]J. R. Klauder, Phys. Rev. D **19**, 2349 (1979).
[36]D. H. Lee and M. P. A. Fisher, Int. J. Mod. Phys. B **5**, 2675 (1991).
[37]G. Delfino and G. Mussardo, Nucl. Phys. B **516**, 675 (1998).
[38]Note that a fine tuning of the modulation may lead to $\mathbb{Z}_3$ criticality, such as the one found in spin-1/2 chain in magnetic field, see P. Lecheminant and E. Orignac, Phys. Rev. B **69**, 174409 (2004).
[39]C. J. Morningstar and M. Weinstein, Phys. Rev. D **54**, 4131 (1996).
[40]S. Capponi, A. Läuchli, and M. Mambrini, Phys. Rev. B **70**, 104424 (2004).
[41]A. Abendschein and S. Capponi, Phys. Rev. B **76**, 064413 (2007).
[42]In the case where both cosines are in competition, an exotic criticality can emerge. See, for example, P. Lecheminant, A. O. Gogolin, and A. A. Nersesyan, Nucl. Phys. B **639**, 502 (2002).
[43]In this staggered spin-imbalance phase, two sites per rung have the same magnetization so that reflection symmetry is preserved and the ground state is sixfold degenerate. Note that the presence of a higher harmonic $\cos(12\sqrt{2\pi}\,\tilde{\chi}$ may induce a fully symmetry-broken spin-imbalance phase with all three magnetizations different (i.e., twelvefold-degenerate ground state).
[44]S. R. White, Phys. Rev. Lett. **69**, 2863 (1992).
[45]P. Calabrese and J. Cardy, J. Stat. Mech.: Theor. Exper. (2004) P06002.
[46]For the spin-1/2 tube, a ferrochiral phase has been found in the weak-coupling regime for any finite magnetic field (Ref. 28).
[47]J. Schnack, H. Nojiri, P. Kögerler, G. J. T. Cooper, and L. Cronin, Phys. Rev. B **70**, 174420 (2004).
[48]J.-B. Fouet, A. Läuchli, S. Pilgram, R. M. Noack, and F. Mila, Phys. Rev. B **73**, 014409 (2006).
[49]N. B. Ivanov, J. Schnack, R. Schnalle, J. Richter, P. Kögerler, G. N. Newton, L. Cronin, Y. Oshima, and H. Nojiri, Phys. Rev. Lett. **105**, 037206 (2010).
[50]D. C. Cabra, A. De Martino, A. Honecker, P. Pujol, and P. Simon, Phys. Rev. B **63**, 094406 (2001).
[51]D. C. Cabra, A. D. Martino, P. Pujol, and P. Simon, Europhys. Lett. **57**, 402 (2002).
[52]C. A. Lamas, S. Capponi, and P. Pujol, Phys. Rev. B **84**, 115125 (2011).
[53]V. Subrahmanyam, Phys. Rev. B **52**, 1133 (1995).
[54]F. Mila, Phys. Rev. Lett. **81**, 2356 (1998).
[55]Y. Kamiya and C. D. Batista, Phys. Rev. Lett. **108**, 097202 (2012).